

RAPID COMMUNICATIONS

The purpose of this Rapid Communications section is to provide accelerated publication of important new results in the fields regularly covered by *Journal of Materials Research*. Rapid Communications cannot exceed four printed pages in length, including space allowed for title, figures, tables, references, and an abstract limited to about 100 words.

Giant pop-ins in nanoindented silicon and germanium caused by lateral cracking

D.J. Oliver^{a)}

Department of Electronic Materials Engineering, Research School of Physical Sciences and Engineering, The Australian National University, Canberra ACT 0200, Australia

B.R. Lawn, R.F. Cook, and M.G. Reitsma

Materials Science and Engineering Laboratory, National Institute of Standards and Technology, Gaithersburg, Maryland 20899

J.E. Bradby and J.S. Williams

Department of Electronic Materials Engineering, Research School of Physical Sciences and Engineering, The Australian National University, Canberra ACT 0200, Australia

P. Munroe

Electron Microscope Unit, University of New South Wales, Sydney, NSW 2052, Australia

(Received 16 September 2007; accepted 16 November 2007)

Giant “pop-in” displacements are observed in crystalline silicon and germanium during high-load nanoindentation with a spherical diamond tip. These events are consistent with material removal triggered by lateral cracking during loading, which poses a hazard to microelectromechanical systems (MEMS) operation. We examine the scaling of the pop-in displacements as a function of peak indentation load and demonstrate a correlation with the depth of the plastic contact zone. We argue that giant pop-ins may occur in a broad range of highly brittle materials.

Silicon (Si) and germanium (Ge) are basic Group IV semiconducting materials widely used in electronics, integrated circuitry, and microelectromechanical systems (MEMS) and nanoelectromechanical systems (NEMS) devices. The two materials have the same crystal structure and are highly brittle with similar mechanical properties, including hardness, H , and fracture toughness, K_{IC} (Table I). They show similar responses on indentation with sharp tips, with well-defined hardness impressions accommodated by punching-in of dislocated shear faults immediately beneath the contact at high stresses.^{1,2} Some differences are also evident: in Si, deformation is additionally accommodated by a surface-localized pressure-induced phase transformation to a dense, metallic Si-II phase^{3,4}; in Ge, there is evidence of accompanying mechanical twinning within the shear fault zone.^{5,6} The net result is an approximately hemispherical plastic impression beneath the indent,⁷ containing nucleation sources for ensuing crack initiation and propagation.^{8–11}

Over the past two decades, much attention has been given to the use of depth-sensing nanoindentation to characterize mechanical properties of a wide range of materials. It is well documented that both hardness and Young's modulus can be extracted from the indentation force–displacement (P – h) responses.⁶ More recently, discontinuities in the displacement responses, known as pop-ins, have been studied as markers of abrupt deformation events during indentation. These include the onset of abrupt slip,¹² phase transformation,¹³ and radial fracture.¹⁴ The pop-ins are usually small, on the order of 10–50 nm. However, in bulk crystalline Ge, much larger displacements, in excess of 1 μm , have recently been observed.⁶ These “giant” pop-ins are attributed to lateral cracks which initiate within the quasiplastic zone and spread sideways into a saucer-like configuration, ultimately intersecting the surface to produce a spall.¹⁵ Such spalls are generally accompanied by particulate debris around the indent site.⁶ The nature of such spalling damage at small-scale contacts demands attention because of the potential for highly adverse effects on MEMS device operation.^{16–18}

Nanoindentation has been used previously to study indentation fracture, typically using pyramidal (four-sided

^{a)}Address all correspondence to this author.

e-mail: djo109@rsphysse.anu.edu.au

DOI: 10.1557/JMR.2008.0070

TABLE I. Properties of Si and Ge, taken from Ref. 2.

Material	H (GPa)	K_c (MPa·m ^{1/2})	H/K_c (μm ^{1/2})
Si	9	0.7	12.9
Ge	8	0.6	13.3

Vickers or three-sided Berkovich) indenter tips. The fracture response under a pyramidal indenter differs somewhat to the response under a spherical indenter: stress is intensified at the sharp edges of the pyramidal indenter, favoring the radial cracking mode and tending to cause cracking at lower applied loads.¹⁹ Cook has given an overview of indentation fracture in silicon.¹¹ Fracture events may be manifested in the P - h response as pop-ins or changes in slope.²⁰⁻²² Field et al. have proposed that the magnitude of pop-ins induced by radial fracture may be used to determine fracture toughness in some systems.¹⁴

To gain a better understanding of the underlying micromechanics of giant pop-in events, we have conducted comparative nanoindentation experiments on Si and Ge over a broad range of maximum loads. Highly polished wafers of single-crystal Si (Unisil Corp., Santa Clara, CA) and Ge (Wafer World, West Palm Beach, FL) with (100) surfaces were indented using a spheroconical tip of radius 4.3 μm using the UMIS-2000 nanoindenter (CSIRO, Sydney, Australia). Maximum loads up to 900 mN were used, attained in 225 loading increments, at loading and unloading rates $dP/dt \approx 1.5 \text{ mN}\cdot\text{s}^{-1}$, and P - h curves recorded. For statistical analysis, 20×20 arrays of indents were created in each specimen surface. Pop-in displacements were extracted from the resulting P - h datasets.

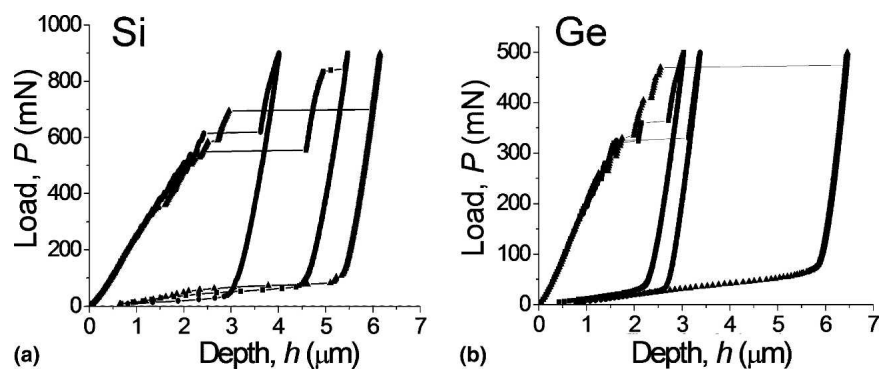
Indents were cross sectioned using a dual-beam focused ion beam (FIB) microscope (FEI xT Nova Nanolab 200, Hillsboro, OR) to examine subsurface cracking, as detailed previously.⁶ Prior to ion milling, a thin film of platinum was deposited to protect the indents from ion-beam damage. Top surface views and cross sections were imaged using the electron beam at a tilt angle of 52°.

Representative P - h curves are shown in Fig. 1 for

maximum loads (a) 900 mN in Si and (b) 500 mN in Ge. At these loads the curves all feature giant displacement pop-ins, indicated by the near-horizontal traces in the plots. The magnitudes of the displacement increments range up to $\sim 5 \mu\text{m}$ in both materials under the loading conditions shown. The loads at which pop-in first occurs, and the resulting displacements, vary considerably from test to test, indicating some stochastic in the pop-in micromechanics.

Figure 2 shows top-surface and cross-section images of indents in Si and Ge that have undergone giant pop-ins. Well-defined hardness impressions are observed at the indentation centers, consistent with contacts in the plastic region. Extensive cracking is apparent around the indentation sites, with radial and lateral cracking. From the cross-section views, the lateral cracks initiate from the plastic zone, at depths somewhere between the top surface and the zone base. These cracks run approximately parallel to the top surface, in some cases propagating all the way upward to the surface to produce scallop-shaped chip segments confined within preceding radial cracks.¹⁵ All indents with giant pop-ins revealed one or more such segments, suggesting a correlation between spallation and displacement increment. Note debris particles around the indents in Figs. 2(a) and 2(b). The extent of this debris was shown previously for Ge to correlate with pop-in size.⁶

To quantify this behavior, Fig. 3 plots pop-in displacement h_* as a function of corresponding critical indentation load P_* (inset) for Si and Ge. Notwithstanding the scatter in data, there appear to be definable threshold loads, $P_C \approx 350 \pm 100 \text{ mN}$ for Si and $P_C \approx 250 \pm 80 \text{ mN}$ for Ge (vertical dashed lines), above which pop-ins occur, as determined by visual inspection. The pop-in displacements h_* show considerable variation but are more or less bound by upper envelopes (solid lines). These envelopes are derived simplistically from the standard hardness relation $H = P_*/\pi a^2$, with a the contact radius, by equating the maximum displacement with the plastic zone depth to obtain $h_* \approx a_* = (P_*/\pi H)^{1/2}$, using H values from Table I. Because H for Si and Ge are within

FIG. 1. P - h curves for (a) Si to 900 mN and for (b) Ge to 500 mN.

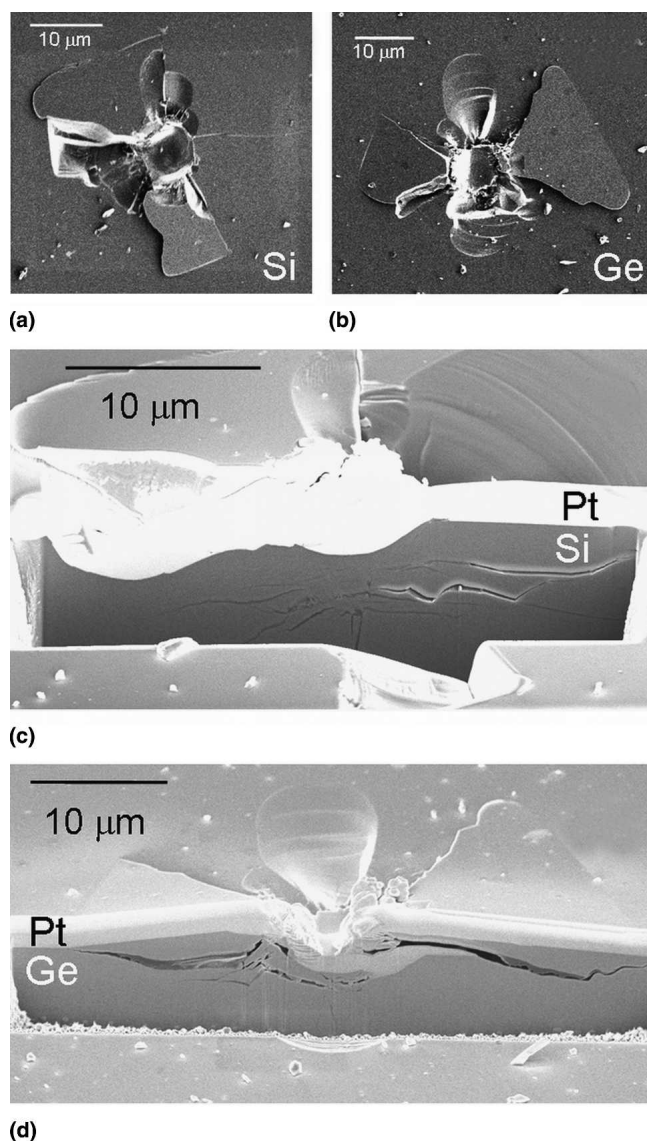


FIG. 2. Top-down and cross-sectional FIB images of indents in Ge and Si that have undergone a giant pop-in: (a, c) 550-mN indent in Si; (b, d) 350-mN indent in Ge.

10% of each other, the predicted envelopes in Figs. 3(a) and 3(b) differ only slightly.

Interestingly, some of the data for Ge fall slightly above the envelope, while all the data for Si fall somewhat below the envelope. That is to say, the pop-ins for Si are somewhat smaller than the model would indicate, suggesting that none of the lateral cracks in Si initiate at the very base of the plastic zone but instead are somewhat shallower, resulting in less material removal. We suggest two possible reasons for this, both related to the occurrence of phase transformation as the dominant inelastic deformation mechanism in Si. The densification inherent in the pressure-induced phase transformation has the effect of lowering the driving stress field for cracking,²³ analogous to the effect of densification on

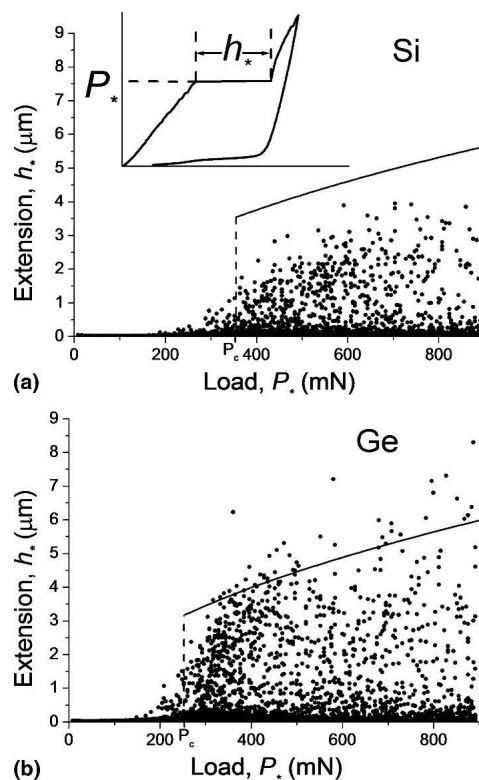


FIG. 3. Pop-in size as a function of pop-in load for (a) Si and (b) Ge. Points are experimental data. The solid line is the indenter contact radius, calculated from $\alpha_* = (P_*/\pi H)^{1/2}$. (Inset) Schematic showing P_* and h_* .

cracking morphology in anomalous glasses.²⁴ Additionally, with less shear plasticity in Si, there will be a lower density of shear defects and less interaction between defects, limiting the number of flaw sites available for crack nucleation^{6,9}; the sites are also likely to lie closer to the surface, reducing the depth of crack initiation. This is consistent with the view that Si deforms predominantly by pressure-induced phase transformation,^{3,4} whereas Ge deforms predominantly by shear plasticity.^{5,6}

It is instructive to elaborate on the micromechanics of the envisioned pop-in process. Entering the plastic region, the indentation generates dislocated shear bands or flaws that act as precursors for lateral (and radial) cracks. The shear events are discrete at the submicron level and so become subject to statistical distributions at low contact loads.⁶ At higher loads, the spatial extent of the flaws increases, in proportion to the characteristic contact dimension a , without significantly increasing the stress intensity acting on these flaws (i.e., load-independent hardness).^{8,9} The depth of the ensuing lateral cracks that grow out of the flaws also scales with a , as indicated in the above derivation of the envelope curves in Fig. 3. Once a lateral crack intersects the surface, it is on the verge of detachment, thus reducing the support on the indenter. In some cases the lateral cracks will initiate close to the base of the plastic zone, in others somewhere between the

base and the top surface, depending on the stochastics. Hence the envelopes in Fig. 3 represent an upper bound and account for the wide scatter in data within those envelopes. Lateral chips that have not been detached will act as levers and contribute to recovery on unloading, accounting for the elbowing observed on unloading and consequent depth recovery.⁶

It remains to account for the small but seemingly significant differences observed in the critical threshold loads for Si and Ge. An earlier fracture mechanics analysis of radial cracks gives a simple relation for threshold load, $P_c \propto K_c^4/H^3$, with hardness H and toughness K_c given in Table I.⁸ This relation predicts a 30% higher value of P_c for Si than for Ge, which compares with a ~40% higher value in Fig. 3. Thus, allowing for the data scatter and the sensitivity of P_c to small variations in K_c and H in the threshold relation, the results appear to be consistent qualitatively and quantitatively with a lateral crack spallation model.

Although the lateral cracking described here occurs during loading, it is more commonly observed during unloading, because the elastic stress field under the loaded indenter tends to suppress it.¹⁵ While lateral cracking on unloading will not cause a giant pop-in it seems probable that, after it has formed on unloading, subsequent reloading may trigger giant pop-in and material removal. Indeed, Cook and Pharr reported large displacements on reloading of sapphire,²³ connected with lateral crack spallation, and we have observed giant pop-ins on repeated loading in Ge at lower loads than during single loading,²⁵ suggesting that repeated contact events increase the likelihood of material removal.

We would argue that the giant pop-in events described here are not specific to Si or Ge, but could apply to any highly brittle material. By highly brittle, we mean materials with low threshold loads P_c , specifically materials with large values of H/K_c , the so-called “brittleness index.”¹⁰ Si and Ge fall into the upper range of brittleness, due to their highly covalent bonding. Other candidate materials are diamond, silicon carbide, sapphire, silicon nitride, III–V semiconductors, and some glasses. Giant pop-ins have also been observed in thin-film systems.²⁶ In these latter systems, an additional trigger for spallation is film delamination along a weakly adhering interface, in which case the pop-in displacement may be governed more by film thickness than by plastic zone size.

This work also confirms that fractures associated with sharp-contact events can generate particulate debris. In MEMS devices, contact events that do not directly impact the working elements of a device may nevertheless generate debris that interferes with operation.^{16–18} Shock¹⁶ or vibration¹⁸ loading during device operation could transport such debris to inter-element locations, causing mechanical jamming or electrical shorting. The single-contact induced fragments observed here are typi-

cally larger than the wear particles generated during operation of MEMS devices,^{16,18} where device failure is associated with material removal leading to a loss of element dimensional tolerance. In such cases, the wear particles are a symptom, not a cause, of device failure. The observations here suggest that debris generation may be minimized by avoiding sharp contacts, thereby improving device reliability.

ACKNOWLEDGMENT

This work was supported by a travel grant from the Australian Research Network for Advanced Materials. Certain commercial equipment, instruments, or materials are identified in this paper. Such identification does not imply recommendation or endorsement by the National Institute of Standards and Technology.

REFERENCES

1. S.V. Hainsworth, A.J. Whithead, and T.F. Page: The nanoindentation response of silicon and related structurally similar materials, in *Plastic Deformation of Ceramics*; edited by R.C. Bradt, C.A. Brookes, and J.L. Routbort (Plenum: New York, 1995), p. 173.
2. B.R. Lawn, B.J. Hockey, and S.M. Wiederhorn: Atomically sharp cracks in brittle solids: An electron microscopy study. *J. Mater. Sci.* **15**(5), 1207 (1980).
3. D.R. Clarke, M.C. Kroll, P.D. Kirchner, R.F. Cook, and B.J. Hockey: Amorphization and conductivity of silicon and germanium induced by indentation. *Phys. Rev. Lett.* **60**(21), 2156 (1988).
4. J.E. Bradby, J.S. Williams, J. Wong-Leung, M.V. Swain, and P. Munroe: Transmission electron microscopy observation of deformation microstructure under spherical indentation in silicon. *Appl. Phys. Lett.* **77**(23), 3749 (2000).
5. J.E. Bradby, J.S. Williams, J. Wong-Leung, M.V. Swain, and P. Munroe: Nanoindentation-induced deformation of Ge. *Appl. Phys. Lett.* **80**(15), 2651 (2002).
6. D.J. Oliver, J.E. Bradby, J.S. Williams, M.V. Swain, and P. Munroe: Giant pop-ins and amorphization in germanium during indentation. *J. Appl. Phys.* **101**(4), 043524 (2007).
7. L.E. Samuels and T.O. Mulhearn: An experimental investigation of the deformed zone associated with indentation hardness impressions. *J. Mech. Phys. Solids* **5**(2), 125 (1957).
8. B.R. Lawn and A.G. Evans: A model for crack initiation in elastic/plastic indentation fields. *J. Mater. Sci.* **12**(11), 2195 (1977).
9. J.T. Hagan: Micromechanics of crack nucleation during indentations. *J. Mater. Sci.* **14**(12), 2975 (1979).
10. B.R. Lawn and D.B. Marshall: Hardness, toughness, and brittleness: An indentation analysis. *J. Am. Ceram. Soc.* **62**(7–8), 347 (1979).
11. R.F. Cook: Strength and sharp contact fracture of silicon. *J. Mater. Sci.* **41**(3), 841 (2006).
12. D. Lorenz, A. Zeckzer, U. Hilpert, P. Grau, H. Johansen, and H.S. Leipner: Pop-in effect as homogeneous nucleation of dislocations during nanoindentation. *Phys. Rev. B* **67**(17), 172101 (2004).
13. E.R. Weppelmann, J.S. Field, and M.V. Swain: Observation, analysis, and simulation of the hysteresis of silicon using ultramicro-indentation with spherical indenters. *J. Mater. Res.* **8**(4), 830 (1993).

14. J.S. Field, M.V. Swain, and R.D. Dukino: Determination of fracture toughness from the extra penetration produced by indentation-induced pop-in. *J. Mater. Res.* **18**(6), 1412 (2003).
15. D.B. Marshall, B.R. Lawn, and A.G. Evans: Elastic plastic indentation damage in ceramics—the lateral crack system. *J. Am. Ceram. Soc.* **65**(11), 561 (1982).
16. D.M. Tanner, J.A. Walraven, K.S. Helgesen, L.W. Irwin, F. Brown, N.F. Smith, and N. Masters: MEMS reliability in a shock environment, in *Proceedings of the 38th Annual IEEE International Reliability Physics Symposium*, 2000, pp. 129–138.
17. J.A. Walraven: Failure mechanisms in MEMS, in *Test Conference, 2003. Proceedings of the International Test Conference (ITC)*, 2003, Vol. 1, pp. 828–833.
18. T.F. Tan, K. Weber, and C.K.H. Dharan: Failure analysis of thermal actuators, comb drives, and other microelectromechanical elements. *J. Failure Anal. Prevent.* **7**, 137 (2007).
19. M.V. Swain and M. Wittling: Comparison of acoustic emission from pointed and spherical indentation of TiN films on silicon and sapphire. *Surf. Coat. Technol.* **76–77**, 528 (1995).
20. S.V. Hainsworth, M.R. McGurk, and T.F. Page: The effect of coating cracking on the indentation response of thin hard-coated systems. *Surf. Coat. Technol.* **102**(1–2), 97 (1998).
21. E.G. Berasategui and T.F. Page: The contact response of thin SiC-coated silicon systems—Characterisation by nanoindentation. *Surf. Coat. Technol.* **163–164**, 491 (2003).
22. R. Rabe, J.M. Breguet, P. Schwaller, S. Stauss, F.J. Haug, J. Patscheider, and J. Michler: Observation of fracture and plastic deformation during indentation and scratching inside the scanning electron microscope. *Thin Solid Films* **469–470**, 206 (2004).
23. R.F. Cook and G.M. Pharr: Direct observation and analysis of indentation cracking in glasses and ceramics. *J. Am. Ceram. Soc.* **73**(4), 787 (1990).
24. A. Arora, D.B. Marshall, B.R. Lawn, and M.V. Swain: Indentation deformation/fracture of normal and anomalous glasses. *J. Non-Cryst. Solids* **31**(3), 415 (1979).
25. D.J. Oliver, J.E. Bradby, J.S. Williams, M.V. Swain, D. McGrouther, and P. Munroe: Indentation-induced damage mechanisms in germanium, in *Focused Ion Beams for Analysis and Processing*, edited by W. MoberlyChan, H. Colijn, R. Langford, and A. Marshall (Mater. Res. Soc. Symp. Proc. **983E**, Warrendale, PA, 2007), 0983-LL08-02.
26. C.M. Lepienski, M.D. Michel, P.J.G. Araujo, and C.A. Achete: Indentation fracture of *a*-C:H thin films from chemical vapour deposition. *Philos. Mag.* **86**(33–35), 5397 (2006).